

## Article

# Investigation of Calcium and Magnesium Phosphate Crystals in Stones Treated with Diammonium Hydrogen Phosphate Conservation Product: Potential of Micro-Raman Spectroscopy

Claudia Conti <sup>1,\*</sup>, Léa Cutard <sup>2</sup>, Alessandra Botteon <sup>1</sup>, Luigi Brambilla <sup>3</sup>, Nicoletta Marinoni <sup>4</sup>, Marco Realini <sup>1</sup>, Maria Catrambone <sup>1</sup>, Elena Possenti <sup>1</sup> and Chiara Colombo <sup>1,\*</sup>

<sup>1</sup> Institute of Heritage Science (ISPC), National Research Council (CNR), 20125 Milan, Italy; alessandra.botteon@cnr.it (A.B.); marco.realini@cnr.it (M.R.); maria.catrambone@cnr.it (M.C.); elena.possenti@cnr.it (E.P.)

<sup>2</sup> UFR de Chimie, Faculté des Sciences et Ingénierie, Sorbonne Université, 75005 Paris, France; lea.cutard@etu.sorbonne-universite.fr

<sup>3</sup> Department of Chemistry, Materials and Chemical Engineering Giulio Natta, Politecnico di Milano, 20133 Milan, Italy; luigi.brambilla@polimi.it

<sup>4</sup> Department of Earth Sciences “Ardito Desio”, Università degli Studi di Milano, 20133 Milan, Italy; nicoletta.marinoni@unimi.it

\* Correspondence: claudia.conti@cnr.it (C.C.); chiara.colombo@cnr.it (C.C.)

**Abstract:** This study is aimed at investigating crystals (calcium and magnesium phosphates) formed due the interaction of an inorganic conservation treatment (diammonium hydrogen phosphate—DAP) with carbonatic (calcitic and dolomitic) stones through micro-Raman Spectroscopy. The addressed questions concern (i) the identification of magnesium and calcium phosphate minerals crystallized within dolomitic stone samples with a different degree of conservation state and treated with two different DAP solution molarities and (ii) the distinction of complex calcium phosphate mixtures (hydroxyapatite—HAP and octa calcium phosphate—OCP) crystallized within a calcarenite stone treated with DAP. A statistically relevant number of Raman spectra have been acquired in sample cross sections and curve fitting analysis has been performed for the in-depth interpretation of data. The outcomes indicate that Raman Spectroscopy is an effective alternative method for the identification of poorly crystalline calcium phosphates (not easily detectable with X-ray diffraction), even when scarcely present in mixture with magnesium phosphates. Evidence of the Raman analytical capability and high potential to distinguish HAP and OCP in calcitic stones are also presented and discussed.

**Keywords:** diammonium hydrogen phosphate; Raman Spectroscopy; dolomite; calcite; calcium phosphate; struvite; conservation treatment



**Citation:** Conti, C.; Cutard, L.; Botteon, A.; Brambilla, L.; Marinoni, N.; Realini, M.; Catrambone, M.; Possenti, E.; Colombo, C. Investigation of Calcium and Magnesium Phosphate Crystals in Stones Treated with Diammonium Hydrogen Phosphate Conservation Product: Potential of Micro-Raman Spectroscopy. *Crystals* **2023**, *13*, 1212. <https://doi.org/10.3390/cryst13081212>

Academic Editor: Juan Ángel Sans

Received: 6 July 2023

Revised: 28 July 2023

Accepted: 1 August 2023

Published: 5 August 2023



**Copyright:** © 2023 by the authors. Licensee MDPI, Basel, Switzerland. This article is an open access article distributed under the terms and conditions of the Creative Commons Attribution (CC BY) license (<https://creativecommons.org/licenses/by/4.0/>).

## 1. Introduction

Stone conservation is a major challenge in Heritage Science. In recent years, treatments based on inorganic products, such as diammonium hydrogen phosphate (DAP— $(\text{NH}_4)_2\text{HPO}_4$ ) have been successfully introduced in conservation to consolidate the decayed microstructure of carbonate stone artefacts. These treatments, based on DAP aqueous solutions, react with carbonates of the stone substrates, and form new crystalline phases (phosphates) via a dissolution–recrystallization process. The crystallization of new phases within the treated stone material gives rise to a novel “stone material-new phases” system with specific properties [1].

Most of the studies focused on the reaction of DAP with calcite (calcium carbonate,  $\text{CaCO}_3$ )-based materials, both natural (stones) and artificial (i.e., plasters, mortars). Ideally, the DAP reaction with calcite should form crystalline hydroxyapatite (HAP,  $\text{Ca}_{10}(\text{PO}_4)_6(\text{OH})_2$ ). However, the DAP reaction in presence of carbonate ions is not stoichiometric and other calcium phosphate phases (CaPs) are formed alongside HAP (i.e., octacalcium phosphate

OCP,  $\text{Ca}_8(\text{HPO}_4)_2(\text{PO}_4)_4 \cdot 5\text{H}_2\text{O}$ ); dicalcium phosphate dihydrate, DCPD,  $\text{CaHPO}_4 \cdot 2\text{H}_2\text{O}$ ; poorly crystalline calcium-deficient HAP; and/or carbonate-substituted HAP) in a complex mixture [2–5]. The crystallochemical composition, the crystallinity of these phases, as well as their spatial distribution within the treated stone materials was found to be strongly dependent on several variables mutually interacting during the DAP reaction. These factors include the physical features of the substrate (its mineralogy, grain size and microstructure), as well as the treatment modalities (i.e., DAP molarity, treatment duration, application methods, pH, ionic strength during the DAP reaction) [5–8].

The formation of specific crystalline phases (each of them with peculiar properties, i.e., stability, solubility) in specific areas of the treated stone material influences the effects induced by the consolidation treatment on the substrate [9]. Understanding the mechanisms ruling the reaction is a key point to optimize the effectiveness of DAP treatments as a function of specific conservation needs. To do that, an exhaustive characterization of the crystallochemical composition and spatial distribution of reaction products is strongly needed.

The identification of CaPs is very challenging in all carbonate substrates, as demonstrated by several studies [5,10,11]. In fact, the new phases are poorly-crystalline, in complex mixtures and in low amount compared to the minerals of the substrate. In addition, many of them have similar elemental composition and crystal structure. In particular, distinguishing HAP from OCP (and from the other apatite-like CaPs) is a real analytical challenge as the apatite-like crystal structure of OCP is deeply similar to the HAP crystalline arrangement; thus, both of them give rise to severe overlapping of X-ray diffraction peaks [3,4,9].

The dissolution–recrystallization reaction is different when DAP treatments are applied to Mg-containing carbonate matrices, such as with dolomite (magnesium calcium carbonate,  $\text{MgCa}(\text{CO}_3)_2$ ) of dolomitic veins in marbles and dolostones. In case of DAP treatments applied to polycrystalline dolomite, the high Mg content within the stone material promotes the crystallization of a final phase assemblage different from that observed on calcite-based materials and mainly magnesium phosphate phases (MgPs) are formed [3,10]. However, the topic concerning the interaction between DAP and Mg-containing stone substrates still needs to be explored in depth.

Moreover, no data are available on the effects induced by DAP treatments when applied to carved and decayed stone, by exposure to outdoor conditions as in case of historical buildings, dolostones. This is a crucial point as the DAP reaction with a decayed dolostone (and the descending crystallization) may be different from that occurring with quarry specimens, since other factors (such as the increase of porosity in decayed microstructures, higher specific surface area, corrosion of dolomitic grains due to decay, or presence of other phases or soluble salts) are expected to participate or influence the formation of specific phases.

Based on this context, with the present research we explored micro-Raman spectroscopy and characterized by intrinsic high chemical selectivity and high lateral resolution, as an effective tool for studying the crystallochemical composition and the spatial distribution of phosphate phases occurring after DAP treatments of a dolomitic stone (Angera stone). To the best of our knowledge, this topic has not been explored in the dolomitic matrix yet, and only a few data are available for calcitic substrates [12]. The study is carried out on quarry and decayed specimens of Angera stone with the aim of understanding the possible differences in terms of the composition and distribution of MgPs and CaPs phases (crystalline and poorly crystalline new compounds), as a function of the microstructural peculiarities of the different stone substrates and DAP treatment modalities. The potential of Raman is explored to boost the characterization of poorly crystalline CaPs phases, to ascertain the simultaneous formation of HAP and OCP, in the perspective of overcoming the intrinsic XRD limitations in the identification of these phases.

## 2. Materials and Methods

Concerning the reference powders, HAP was purchased from Sigma-Aldrich and OCP was synthesized in the laboratory as reported in [3] by modifying the LeGeros procedure [13].

Samples S1, S2, S3, and S4 correspond to Angera stone samples (Table 1). The Angera stone is a dolostone quarried in the northern Italy (Maggiore Lake shore) and has been widely used in the Lombard architecture as an ornamental building material since the Roman age. The lithotype is characterized by a very fine grain size and a high porosity (18–26%, depending on the Angera stone variety) [14]. The stone is mainly composed of dolomite ( $\text{CaMg}(\text{CO}_3)_2$ ) in association with a low fraction of clay minerals and iron oxides. The experiments were performed on the white variety of Angera stone, as this variety undergoes severe decay processes in environmental conditions. Samples S2 and S4 correspond to freshly quarried prismatic samples (50 mm × 50 mm × 20 mm) of Angera stone. Samples S1 and S3 correspond to decayed Angera stone coming from Richini's Court in Ca'Granda, a historical building in Milan (Italy) which dates back to the seventeenth century. The S1, S2, S3, and S4 samples were treated by a 0.76 M or 3 M aqueous solutions of DAP (diammonium hydrogen phosphate), as reported in Table 1. The concentration 0.76 M (corresponding to a 10% *w/w*) was selected based on previous experiments and on the consolidating practice in conservation worksites; the choice to also include 3 M concentration was suggested in previous studies available in the literature, where this value was used to enhance the crystallization of calcium phosphates. The consolidating DAP solution was applied by poultice (dry cellulose pulp, MH 300 Phase, Italy; ratio ~5:1 DAP solution: dry cellulose pulp), as it is one of the most common application methods in the conservation field. The treatment time was 48 h, during which the samples were wrapped in a plastic film to avoid the evaporation of the solvent. After 48 h, the plastic film was removed, and the samples were left drying at room temperature for other 24 h with the poultice on top. The DAP poultice was then removed, and the samples were rinsed three times by applying a novel poultice made with dried cellulose pulp and deionized water; at the end, the stone samples were dried at room temperature.

**Table 1.** Description of the samples. Label, type of stone, and its main mineral, molarity, and application methods of DAP treatment.

Label	Type of Stone	Matrix Mineral	DAP Molarity	DAP Application Method
S1	Angera (decayed)	dolomite	3 M	Poultice—48 h
S2	Angera (quarry)	dolomite	3 M	Poultice—48 h
S3	Angera (decayed)	dolomite	0.76 M	Poultice—48 h
S4	Angera (quarry)	dolomite	0.76 M	Poultice—48 h
S5	Noto (quarry)	calcite	0.76 M	Capillarity—2 h

Sample S5 corresponds to a Noto freshly quarried sample. The Noto limestone is a calcarenite outcropping in the Val di Noto (south-eastern Sicily) used as building stone for the Baroque monuments. Among the several varieties of porous limestones of the Iblean Plateau, the Noto Yellowish Limestone was selected for the study. It is a biomicrite mainly made of calcite, with subordinate clay minerals, quartz, and iron hydroxides, and has high open porosity (25–37%). The consolidating DAP solution was applied by capillarity. The treatment by capillarity was performed putting the sample in contact with 0.76 M DAP water solution through a multiple layer of filter papers (about 1 cm) inside a plastic box for 2 h. The filter papers were inserted dry and they suctioned the consolidating solution by capillarity. The dry sample was then put in contact with the wet surface of the paper filters. During the treatment, the box was kept close to avoid the evaporation of the solvent. After 24 h, the sample was removed from the paper filters and left to dry for 24 h. The sample has been selected since it has been previously analysed by synchrotron X-ray diffraction [11] and the presence of both calcium phosphate phases (HAP and OCP) has been identified.

A small fragment was sampled from each treated stone and cross sections have been prepared by embedding the stone fragments in cold polymerising synthetic resins.

Raman measurements were performed using a Renishaw InVia Qontor spectrometer equipped with a Peltier cooled ( $-70\text{ }^{\circ}\text{C}$ ) NIR enhanced CCD camera and a Leica DM2700 microscope. The excitation wavelength is 785 nm, and 100X (NA 0.85,  $-\text{WD}$  0.3) is the microscope objective used (lateral resolution below  $1\text{ }\mu\text{m}$ ). The laser power was around 12 mW, spectral resolution  $1\text{--}2\text{ cm}^{-1}$ , and spectra range  $100\text{--}1300\text{ cm}^{-1}$ . The total acquisition was 50 s (1 s and 50 accumulations). A confocal pinhole of  $65\text{ }\mu\text{m}$  was used to operate a pure selection of the Raman photons emerging from the focused point; combined with the high lateral resolution, a high degree of confocality was found to be essential for the detection of the phosphates' Raman signal.

The spectra were interpreted using a baseline correction and a normalization to a selected band using OriginPro software. Moreover, a nonlinear curve fitting analysis of the spectra was carried out using Fityk 1.3.1, a free available online software program [15].

XRPD analysis was performed on the bulk samples after DAP treatment. The diffraction patterns were also collected for the corresponding finer sieved fraction (below  $10\text{ }\mu\text{m}$ ), which was obtained through the mechanical sieving of the bulk samples and selecting the surface portion where it was more likely the newly formed phosphate phases were concentrated.

The analyses were performed by a Panalytical X'Pert-PROMPD X'Celerator X-ray powder diffractometer, using Cu  $K\alpha$  radiation ( $\lambda = 1.518\text{ \AA}$ ) at a beam voltage of 40 kV and a current of 40 mA. X-ray powder diffraction patterns were collected over the  $2\text{--}70^{\circ}$  range of the scattering angle  $2\theta$ , with steps of  $0.01^{\circ}$   $2\theta$  and a count time of 50 s per step.

### 3. Results and Discussion

#### 3.1. Diammonium Hydrogenphosphate and Dolomitic Matrix

In the decayed samples, the crystallization of struvite ( $\text{MgNH}_4\text{PO}_4 \cdot 6\text{H}_2\text{O}$ ) appears to be specifically promoted by the 3 M DAP treatment, as is indicated by the appearance of its main diffraction peaks solely in the S1 XRPD pattern (Figure S1). The presence of dicalcium phosphate dihydrate (DCPD, the synthetic analogue of the mineral brushite) in S1 is confirmed through structural refinement using the Rietveld method. This analysis enabled the exclusion of gypsum as an additional accessory phase, which has a peak overlap quite severe with DCPD. Furthermore, it is noteworthy that the S3 sample exhibits a broad hump around 26 and 28 degrees in  $2\theta$  ( $^{\circ}$ ), indicating the presence of an amorphous fraction, likely associated with the neoformation of calcium phosphates (CaPs). As the molarity of the treatment increases, it is observed that within this angular range, a weak and broad diffraction peak appears, confirming the presence of calcium phosphate phases with an increased degree of crystallinity. The situation is different in the samples from the quarry, where the presence of struvite is observed in S2 only, even though at very low concentrations (Figure S2).

An average of 150 Raman spectra have been acquired on each Angera stone cross sections samples (S1–S4) within a depth of about  $150\text{ }\mu\text{m}$ , where there is the highest probability to find intense phosphates bands. Raman spectra provided apparent differences in terms of the newly formed crystals. As can be seen in Figures 1 and S3–S6, besides the dolomite ( $\text{CaMg}(\text{CO}_3)_2$ ) bands ascribed to the stone at  $1098$ ,  $301$  and  $178\text{ cm}^{-1}$ , other Raman signals are present in the spectral range related to the  $\text{PO}_4^{3-}\nu_1$  [16]. The samples decayed and quarry treated with 3 M solution (S1 and S2) unequivocally show a struvite band at around  $950\text{ cm}^{-1}$  [17] in more than 70% of the acquired spectra; a further 6–10% of the spectra exhibit a weak, broad but unambiguously detectable band of calcium phosphate at about  $960\text{ cm}^{-1}$  along with struvite (Figure 2). It is well known that the broader the Raman spectra bandwidth, the lower the degree of mineral crystallinity, thus it is apparent that the broadening of this band is directly related to the low crystalline degree of calcium phosphate, which is likely the reason behind the XRD difficulty of detection.

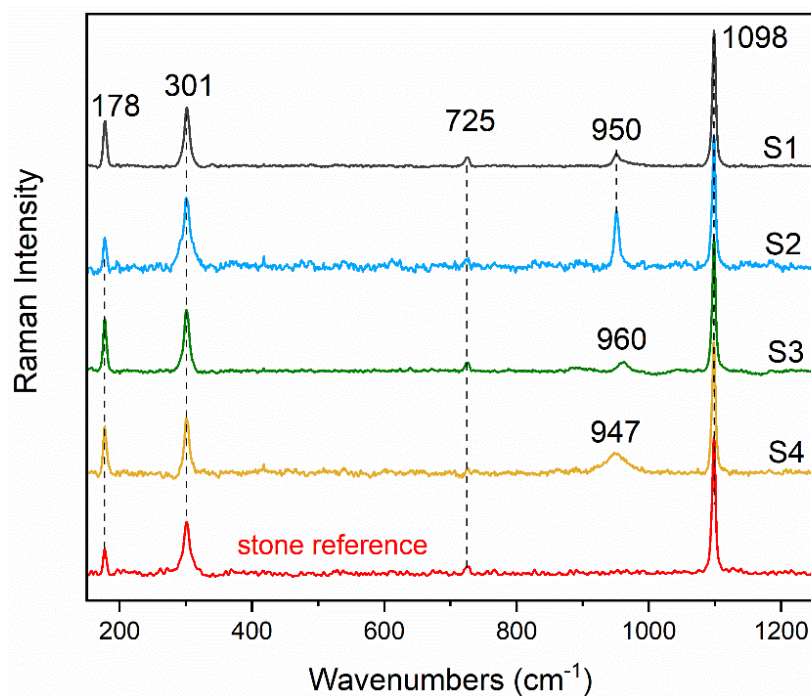


**Figure 1.** Average spectra acquired in S1–S4 samples, normalized to  $1098\text{ cm}^{-1}$  dolomite band. Struvite ( $950\text{ cm}^{-1}$ ) and HAP/OCP ( $960\text{ cm}^{-1}$ ) have been detected along with dolomite ( $1098, 725, 301, 178\text{ cm}^{-1}$ ). Raman spectrum of stone reference is also reported (red spectrum).

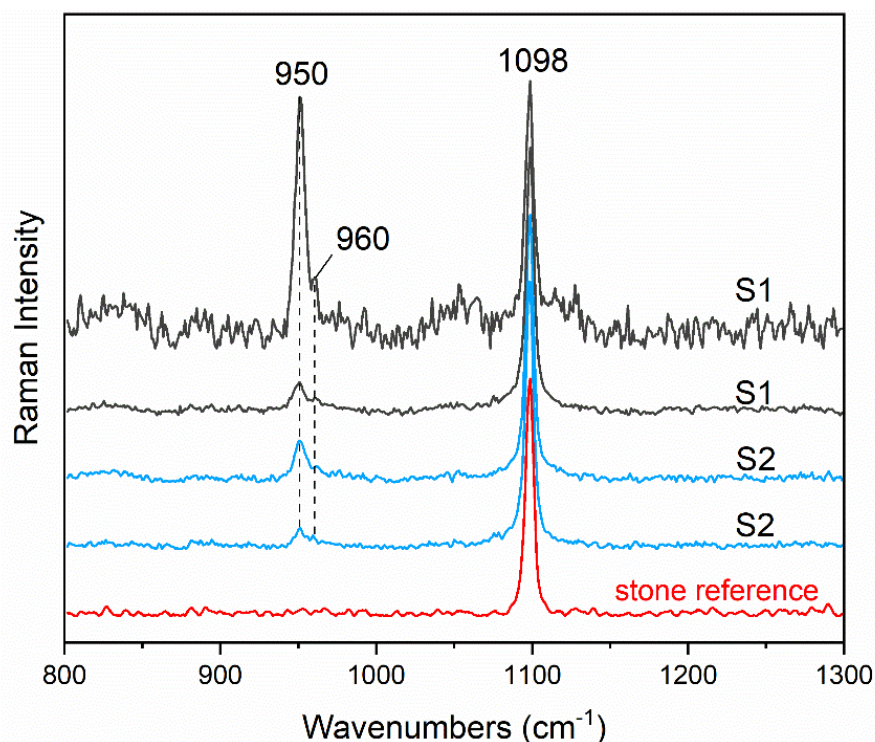


**Figure 2.** Two representative Raman spectra acquired in samples S1 and S2, normalized to  $1098\text{ cm}^{-1}$  dolomite band. HAP/OCP is present ( $960\text{ cm}^{-1}$ ) along with struvite ( $950\text{ cm}^{-1}$ ). Raman spectrum of stone reference is also reported (red spectrum).

A different situation is evidenced in the decayed sample treated with  $0.76\text{ M}$  solution (S3), which does not show the presence of struvite; in about 60% of the spectra a broad band around  $960\text{ cm}^{-1}$  [18] indicates the presence of calcium phosphate in the hydroxyapatite

((Ca<sub>10</sub>(PO<sub>4</sub>)<sub>6</sub>(OH)<sub>2</sub>), HAP) or octacalcium phosphate (Ca<sub>8</sub>(HPO<sub>4</sub>)<sub>2</sub>(PO<sub>4</sub>)<sub>4</sub>·5H<sub>2</sub>O, OCP) in crystalline forms (Figure 1). The quarry sample treated with 0.76 M solution (S4) does not provide significant crystallization of newly formed phases, either struvite or calcium phosphates; only a weak, broad, and unidentified band at about 947 cm<sup>-1</sup> is present (the results are summarized in Table 2).

**Table 2.** Description of main Raman and XRD results in S1–S4 samples. The percentages next to the Raman results are calculated on the total number of the acquired spectra.

	Raman Results		XRPD Results	
	3 M	0.76 M	3 M	0.76 M
Decayed	S1 Struvite (73%) Struvite and HAP/OCP (6%)	S3 HAP/OCP (62%)	S1 Struvite HAP/OCP (traces) DCPD (traces)	S3 Struvite (traces) HAP/OCP (traces)
Quarry	S2 Struvite (72%) Struvite and HAP/OCP (11%)	S4 No Mg and Ca-phosphate	S2 Struvite (traces)	S4 No Mg and Ca-phosphate

The outcomes clearly highlight that in case of 3 M solution, no differences occur in terms of newly formed phases between the decayed and quarry Angera stones; the high concentration of [NH<sub>4</sub><sup>+</sup>] and [PO<sub>4</sub><sup>3-</sup>] along with a source of Mg<sup>2+</sup> ions, as dolomite mineral, can favor struvite crystallization in both cases.

The formation of struvite crystal can be represented by the following reaction:



where n = 0, 1, 2 depends on several factors such as pH, temperature, [Mg<sup>2+</sup>], [NH<sub>4</sub><sup>+</sup>], [PO<sub>4</sub><sup>3-</sup>] and [Ca<sup>2+</sup>]/[Mg<sup>2+</sup>] ratio concentration [19].

The optimal pH for struvite crystallization is in 7.0–7.5 range (90%); however, in the 8.0–8.5 pH range its crystallization is still in the 30–70% range [20,21].

The minimum ratio value [Mg<sup>2+</sup>]/[NH<sub>4</sub><sup>+</sup>]/[PO<sub>4</sub><sup>3-</sup>] for struvite formation is 1:1:1 [19]. Moreover, the literature reports that the presence of calcium in solution inhibits the formation of struvite: the optimal ratio [Ca<sup>2+</sup>]/[Mg<sup>2+</sup>] is 0.5 [22].

As mentioned, Angera stone is mainly composed of dolomite (CaMg(CO<sub>3</sub>)<sub>2</sub>) and its dissolution in water solution is nearly the stoichiometric ratio ([Ca<sup>2+</sup>]/[Mg<sup>2+</sup>] = 1) [22–24]; however, in presence of calcium or phosphate ions in solution, an enrichment of magnesium in solution occurs, up to a ratio of [Ca<sup>2+</sup>]/[Mg<sup>2+</sup>] = 0.32 [24].

Within this context, it is apparent that the application of 3 M DAP solution (pH 8.3) on Angera stone provides two suitable conditions for the crystallization of struvite: ([Mg<sup>2+</sup>]/[NH<sub>4</sub><sup>+</sup>]/[PO<sub>4</sub><sup>3-</sup>] ≥ 1:1:1 and ratio ([Ca<sup>2+</sup>]/[Mg<sup>2+</sup>] ≤ 0.5).

In 0.76 M DAP solution a lower concentration of [NH<sub>4</sub><sup>+</sup>] and [PO<sub>4</sub><sup>3-</sup>] species is present and, although the minimum ratio value [Mg<sup>2+</sup>]/[NH<sub>4</sub><sup>+</sup>]/[PO<sub>4</sub><sup>3-</sup>] is still maintained. The crystallization of calcium and magnesium phosphates is scarce and strongly depends on the conservation state of the stone; in fact, calcium and magnesium phosphates have been detected only in the decayed sample (S3) due to its higher specific surface area which favors the reaction between DAP solution with the matrix.

### 3.2. Diammonium Hydrogenphosphate and Calcitic Matrix

The investigation of OCP and HAP Raman distinction has been carried out using a calcitic stone substrate (Noto limestone) treated with 0.76 M (S5); the cross section has been analyzed within 1 mm in depth acquiring a total of 600 spectra. A strong reaction

between DAP and calcite ( $\text{Ca}(\text{CO}_3)$ ) of the stone occurred, as is demonstrated by the wide diffusion and the intense  $\text{PO}_4^{3-} \nu_1$  bands of newly formed calcium phosphates. The most representative spectra acquired in the stone are shown in Figures 3 and S7 where an intense band at around  $959 \text{ cm}^{-1}$  is present along with the characteristic Raman signals of calcite ( $1086, 712, 282$  and  $156 \text{ cm}^{-1}$ ). Fluorescence originating from the heterogeneous matrix is also present, but it does not affect the readability of the spectra.

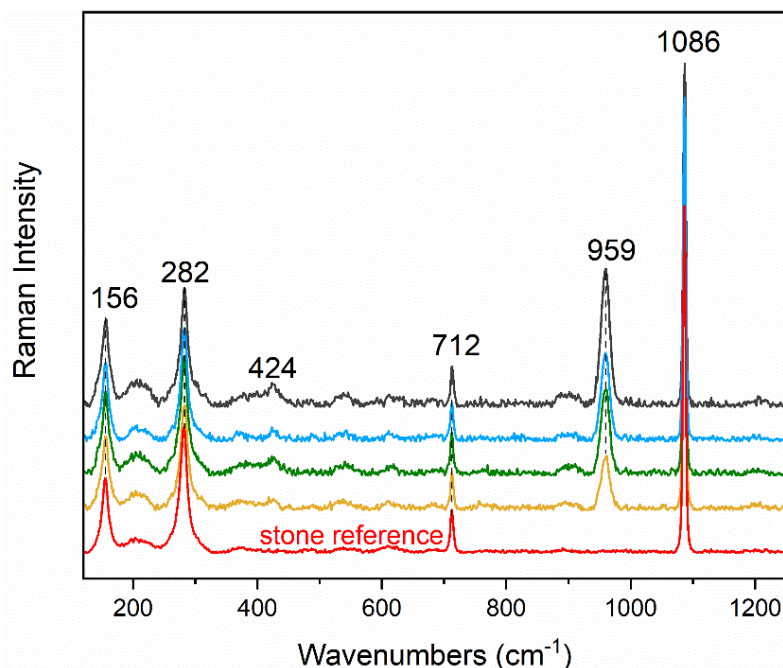


**Figure 3.** Representative Raman spectra acquired in S5, normalized to  $1086 \text{ cm}^{-1}$  calcite band, where the intense  $\text{PO}_4^{3-} \nu_1$  bands of newly formed calcium phosphates are clearly present ( $959$  and  $424 \text{ cm}^{-1}$ ). Raman spectrum of stone reference is also reported (red spectrum).

Reference powders of HAP and OCP have also been analyzed, acquiring 10 spectra for each sample. Moreover, a physical homogeneous mixture of the two powders has been prepared in 50% weight and analyzed (10 spectra). After that, this physical mixture has been intensely ground to study the influence of a reduced crystalline order on the shape and frequency of CaPs bands.

HAP and OCP and mixture spectra are reported in Figure S8. In their pure form, HAP and OCP are easily differentiated due to the  $\text{PO}_4^{3-} \nu_1$  symmetric stretching bands with a frequency of around  $961 \text{ cm}^{-1}$  for HAP and around  $958 \text{ cm}^{-1}$  for OCP. The latter presents a shoulder around  $968 \text{ cm}^{-1}$  as well. In the  $1000\text{--}1100 \text{ cm}^{-1}$ ,  $500\text{--}600 \text{ cm}^{-1}$ , and around  $450 \text{ cm}^{-1}$  spectral ranges the bands ascribed to  $\text{PO}_4^{3-} \nu_3$ ,  $\text{PO}_4^{3-} \nu_4$ , and  $\text{PO}_4^{3-} \nu_2$ , respectively [25,26], would allow a clear distinction between the two phases; however, their intensity is weak and thus it is tricky to detect them when the main  $961\text{--}958 \text{ cm}^{-1}$  band exhibits medium-low intensity.

The curve fitting analysis has been performed for the Raman spectra of the reference materials (HAP and OCP), of the physical mixture (ground and not ground), and of treated Noto stone (S5). The strategy adopted was to search for a solution (deconvoluted spectrum) with a minimum number of individual components. The starting set of Lorentzian and/or Gaussian components were selected according to a supervised analysis of the Raman spectral pattern. The fitting procedure allows for the obtaining of (i) the peak position, (ii) the peak height, (iii) the integrated band area, and (iv) the Full Width at Half Maximum (FWHM) values of each component. In Figure 4 we report the parameters relevant for the discussion, namely peaks position and FWHM, of the components which concur with the main Raman feature ascribed to the convolution of the strong Raman bands of OCP and

HAP  $\text{PO}_4^{3-} \nu_1$ . It is worth noticing that the fitting, performed in the region  $900\text{--}1050\text{ cm}^{-1}$ , often requires the introduction of very broad components to account for the imperfectly straight baseline and some minor Raman bands, which do not contribute to the strong feature around  $960\text{ cm}^{-1}$ .

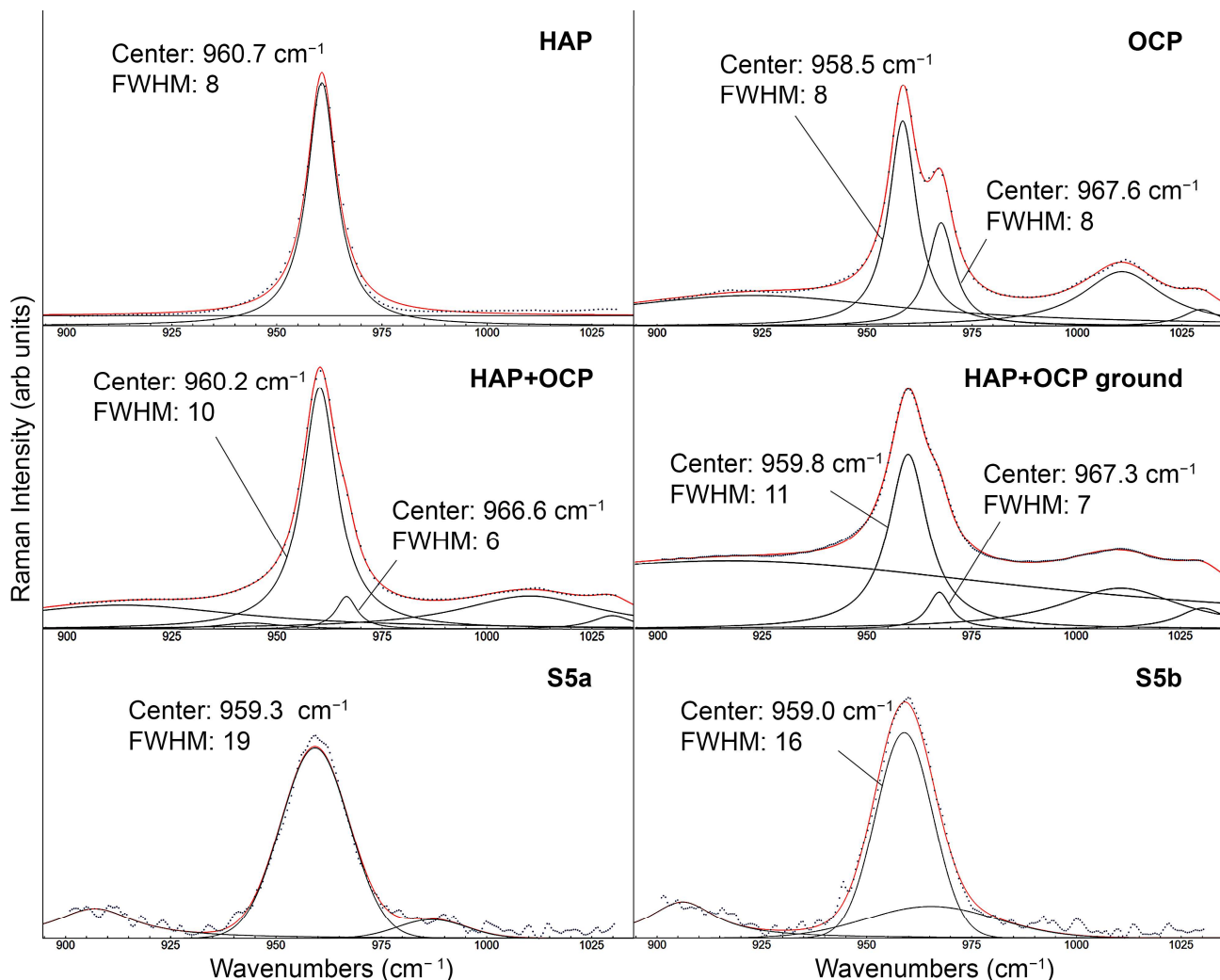


**Figure 4.** Curve fitting analysis of  $\text{PO}_4^{3-}$  symmetric stretching bands of pure reference powders (HAP and OCP), of the physical mixture (not ground and ground), and of treated Noto stone (S5a and S5b). Peak position and Full Width at Half Maximum (FWHM) values are reported for each band discussed in the text. The black dots represent the experimental data while the black and the red lines are the single components and the reconstructed spectrum, respectively.

Very importantly, even if the spectral pattern of the physical mixture of HAP and OCP is exactly the sum of the spectra of two pure components, the curve fitting procedure applied to the physical mixtures does not allow separation of the two main components of HAP and OCP peaking at  $960.7$  and  $958.5\text{ cm}^{-1}$ , since they mainly merge in one only, broader band with Lorentzian shape. A minor component is also present at  $966.6$  and  $967.3\text{ cm}^{-1}$ , related to the OCP second component at  $967.6\text{ cm}^{-1}$ . Interestingly, also in the S5 spectra (S5a and S5b), only one component has been proved with Gaussian shape. Both in terms of frequency and FWHM, S5a and S5b agree more with the OCP and HAP mixture than with the single HAP and OCP phases, supporting the hypothesis of HAP and OCP co-presence. FWHM changes from 8 in pure phases to 10 in the mixture and, after grinding, it increases to 11, demonstrating that grinding produced a slight decrease of the crystalline order. S5 bands exhibit a larger FWHM (16–19), demonstrating that

an even lesser crystalline order exists, which can justify the absence of the minor fitting component at  $966\text{--}967\text{ cm}^{-1}$ ; the shift towards lower wavenumbers can be a consequence of the broadening [27].

#### 4. Conclusions

The strength of micro-Raman spectroscopy on the investigation of newly formed crystals in DAP conservation treatments has been proven. With thanks to its high lateral resolution (below  $1\text{ }\mu\text{m}$ ), confocality condition ( $65\text{ }\mu\text{m}$  pinhole), and intrinsic high chemical selectivity, Raman allowed for the overcoming of conventional X-ray diffraction limitations, through the detection of small amount of poorly crystalline calcium phosphates in mixture with struvite. On the other hand, XRPD bulk analysis is the technique of choice in the case of well-crystallized phases, as struvite which in S3 has been detected only with XRPD.

Moreover, spectral evidence of HAP and OCP co-presence has been extracted by the curve fitting analysis, although some limitations due to severe overlapping of the bands and extensive broadening still need to be faced by combining high lateral resolution and confocality with a higher spectral resolution.

This study sheds light on the complex interactions occurring between the inorganic-mineral treatment and Mg-containing stone material, the role of Mg on the DAP reaction with polycrystalline dolomite substrate and gathers new knowledge about the influence of selected features of the stone substrates (microstructure and content of Mg-ions from Mg-calcite or dolomite) on promoting or inhibiting the formation, localization of stable/metastable, and crystalline/poorly crystalline phases.

**Supplementary Materials:** The following supporting information can be downloaded at: <https://www.mdpi.com/article/10.3390/cryst13081212/s1>, Figure S1: XRPD spectra acquired in samples S1 and S3 (a). Inset of the XRPD patterns (b) where the main diffraction peaks are labeled. DCPD: DCPD; Suv: struvite, Dol: dolomite, CaPs: calcium phosphates, DAP: diammonium hydrogen phosphate. Figure S2 XRPD spectra acquired in samples S2 and S4 (a). Inset of the XRPD patterns (b) where the main diffraction peaks are labeled. Suv: struvite. Figure S3: Representative Raman spectra acquired in samples S1. Struvite band at  $950\text{ cm}^{-1}$  and dolomite at  $1097, 301$  and  $178\text{ cm}^{-1}$  are mainly present. Figure S4: Representative Raman spectra acquired in samples S2. Struvite band at  $950\text{ cm}^{-1}$  and dolomite at  $1097, 301$  and  $178\text{ cm}^{-1}$  are mainly present. Figure S5: Representative Raman spectra acquired in samples S3. HAP/OCP band at  $960\text{ cm}^{-1}$  and dolomite at  $1097, 301$  and  $178\text{ cm}^{-1}$  are mainly present. Figure S6: Representative Raman spectra acquired in samples S4. An unidentified broad band at  $947\text{ cm}^{-1}$  is present, along with dolomite at  $1097, 301$  and  $178\text{ cm}^{-1}$ . Figure S7: Representative Raman spectra acquired in samples S5. HAP/OCP band at  $959\text{ cm}^{-1}$  and calcite at  $1089, 712$  and  $282$  and  $156\text{ cm}^{-1}$  are mainly present. Figure S8: Averaged Raman spectra of reference pure powders (HAP and OCP), of the physical mixture (HAP+OCP) and of the ground physical mixture (HAP+OCP ground). See Figure 4 for the frequency values.

**Author Contributions:** Conceptualization, E.P. and C.C. (Chiara Colombo); Methodology, L.C.; Formal analysis, L.C. and N.M.; Data curation, A.B., L.B. and M.C.; Writing—original draft, C.C. (Claudia Conti), L.C., L.B., N.M., M.C., E.P. and C.C. (Chiara Colombo); Writing—review & editing, C.C. (Claudia Conti), L.C., A.B., L.B., N.M., M.R., M.C., E.P. and C.C. (Chiara Colombo); Supervision, C.C. (Claudia Conti), M.R. and C.C. (Chiara Colombo). All authors have read and agreed to the published version of the manuscript.

**Funding:** This research received no external funding.

**Data Availability Statement:** The data presented in this study are available on request from the corresponding author.

**Conflicts of Interest:** The authors declare no conflict of interest.

## References

1. Hansen, E.; Doehne, E.; Fidler, J.; Larson, J.; Martin, B.; Matteini, M.; Rodriguez-Navarro, C.; Pardo, E.S.; Price, C.; de Tagle, A.; et al. A Review of Selected Inorganic Consolidants and Protective Treatments for Porous Calcareous Materials. *Stud. Conserv.* **2003**, *48* (Suppl. S1), 13–25. [[CrossRef](#)]
2. Matteini, M.; Rescic, S.; Fratini, F.; Botticelli, G. Ammonium Phosphates as Consolidating Agents for Carbonatic Stone Materials Used in Architecture and Cultural Heritage: Preliminary Research. *Int. J. Archit. Herit.* **2011**, *5*, 717–736. [[CrossRef](#)]
3. Possenti, E.; Colombo, C.; Conti, C.; Gigli, L.; Merlini, M.; Plaisier, J.R.; Realini, M.; Sali, D.; Gatta, G.D. Diammonium Hydrogenphosphate for the Consolidation of Building Materials. Investigation of Newly-Formed Calcium Phosphates. *Constr. Build. Mater.* **2019**, *195*, 557–563. [[CrossRef](#)]
4. Wang, L.; Nancollas, G.H. Calcium Orthophosphates: Crystallization and Dissolution. *Chem. Rev.* **2008**, *108*, 4628–4669. [[CrossRef](#)] [[PubMed](#)]
5. Possenti, E.; Colombo, C.; Realini, M.; Song, C.L.; Kazarian, S.G. Time-Resolved ATR–FTIR Spectroscopy and Macro ATR–FTIR Spectroscopic Imaging of Inorganic Treatments for Stone Conservation. *Anal. Chem.* **2021**, *93*, 14635–14642. [[CrossRef](#)] [[PubMed](#)]
6. Celik, S.E.; Gulen, J.; Viles, H.A. Evaluating the Effectiveness of DAP as a Consolidant on Turkish Building Stones. *Constr. Build. Mater.* **2020**, *262*, 120765. [[CrossRef](#)]
7. Molina, E.; Arizzi, A.; Benavente, D.; Cultrone, G. Influence of Surface Finishes and a Calcium Phosphate-Based Consolidant on the Decay of Sedimentary Building Stones Due to Acid Attack. *Front. Mater.* **2020**, *7*. [[CrossRef](#)]
8. Murru, A.; Fort, R. Diammonium Hydrogen Phosphate (DAP) as a Consolidant in Carbonate Stones: Impact of Application Methods on Effectiveness. *J. Cult. Herit.* **2020**, *42*, 45–55. [[CrossRef](#)]
9. Possenti, E.; Conti, C.; Gatta, G.D.; Merlini, M.; Realini, M.; Colombo, C. Synchrotron Radiation  $\mu$ X-ray Diffraction in Transmission Geometry for Investigating the Penetration Depth of Conservation Treatments on Cultural Heritage Stone Materials. *Anal. Methods* **2020**, *12*, 1587–1594. [[CrossRef](#)]
10. Possenti, E.; Conti, C.; Gatta, G.D.; Realini, M.; Colombo, C. Diammonium Hydrogenphosphate Treatment on Dolostone: The Role of Mg in the Crystallization Process. *Coatings* **2019**, *9*, 169. [[CrossRef](#)]
11. Possenti, E.; Conti, C.; Gatta, G.D.; Marinoni, N.; Merlini, M.; Realini, M.; Vaughan, G.B.M.; Colombo, C. Synchrotron X-ray Diffraction Computed Tomography to Non-Destructively Study Inorganic Treatments for Stone Conservation. *iScience* **2022**, *25*, 105112. [[CrossRef](#)]
12. Osticioli, I.; Botticelli, G.; Matteini, P.; Siano, S.; Pini, R.; Matteini, M. Micro-Raman Analysis on the Combined Use of Ammonium Oxalate and Ammonium Phosphate for the Consolidation and Protection of Carbonate Stone Artifacts. *J. Raman Spectrosc.* **2017**, *48*, 966–971. [[CrossRef](#)]
13. LeGeros, R.Z. Preparation of Octacalcium Phosphate (OCP): A Direct Fast Method. *Calcif Tissue Int.* **1985**, *37*, 194–197. [[CrossRef](#)] [[PubMed](#)]
14. Gulotta, D.; Bertoldi, M.; Bortolotto, S.; Fermo, P.; Piazzalunga, A.; Toniolo, L. The Angera Stone: A Challenging Conservation Issue in the Polluted Environment of Milan (Italy). *Environ. Earth Sci.* **2013**, *69*, 1085–1094. [[CrossRef](#)]
15. Wojdyr, M. Fityk: A General-Purpose Peak Fitting Program. *J. Appl. Cryst.* **2010**, *43*, 1126–1128. [[CrossRef](#)]
16. Kirinovic, E.; Leichtfuss, A.R.; Navizaga, C.; Zhang, H.; Schuttlefield Christus, J.D.; Baltrusaitis, J. Spectroscopic and Microscopic Identification of the Reaction Products and Intermediates during the Struvite ( $\text{MgNH}_4\text{PO}_4 \cdot 6\text{H}_2\text{O}$ ) Formation from Magnesium Oxide ( $\text{MgO}$ ) and Magnesium Carbonate ( $\text{MgCO}_3$ ) Microparticles. *ACS Sustain. Chem. Eng.* **2017**, *5*, 1567–1577. [[CrossRef](#)]
17. Lu, B.; Kiani, D.; Taifan, W.; Barauskas, D.; Honer, K.; Zhang, L.; Baltrusaitis, J. Spatially Resolved Product Speciation during Struvite Synthesis from Magnesite ( $\text{MgCO}_3$ ) Particles in Ammonium ( $\text{NH}_4^+$ ) and Phosphate ( $\text{PO}_4^{3-}$ ) Aqueous Solutions. *J. Phys. Chem. C* **2019**, *123*, 8908–8922. [[CrossRef](#)]
18. Karampas, I.A.; Kontoyannis, C.G. Characterization of Calcium Phosphates Mixtures. *Vib. Spectrosc.* **2013**, *64*, 126–133. [[CrossRef](#)]
19. Le Corre, K.S.; Valsami-Jones, E.; Hobbs, P.; Parsons, S.A. Phosphorus Recovery from Wastewater by Struvite Crystallization: A Review. *Crit. Rev. Environ. Sci. Technol.* **2009**, *39*, 433–477. [[CrossRef](#)]
20. Hao, X.; Wang, C.; van Loosdrecht, M.C.M.; Hu, Y. Looking Beyond Struvite for P-Recovery. *Environ. Sci. Technol.* **2013**, *47*, 4965–4966. [[CrossRef](#)] [[PubMed](#)]
21. Hao, X.-D.; Wang, C.-C.; Lan, L.; van Loosdrecht, M.C.M. Struvite Formation, Analytical Methods and Effects of PH and  $\text{Ca}^{2+}$ . *Water Sci. Technol.* **2008**, *58*, 1687–1692. [[CrossRef](#)]
22. Perwitasari, D.S.; Muryanto, S.; Jamari, J.; Bayuseno, A.P. Crystallization of Struvite in the Presence of Calcium Ions: Change in Reaction Rate, Morphology and Chemical Composition. *Cogent Eng.* **2022**, *9*, 2049962. [[CrossRef](#)]
23. Pokrovsky, O.S.; Schott, J. Kinetics and Mechanism of Dolomite Dissolution in Neutral to Alkaline Solutions Revisited. *Am. J. Sci.* **2001**, *301*, 597–626. [[CrossRef](#)]
24. Veetil, S.P.; Mucci, A.; Arakaki, T. Dolomite Dissolution in Aqueous Solutions in the Presence of Nucleotides and Their Structural Components at 25 °C and  $\text{PCO}_2 \sim 1\text{atm}$ . *Chem. Geol.* **2017**, *465*, 64–74. [[CrossRef](#)]
25. Nelson, D.G.A.; Williamson, B.E. Low-Temperature Laser Raman Spectroscopy of Synthetic Carbonated Apatites and Dental Enamel. *Aust. J. Chem.* **1982**, *35*, 715–727. [[CrossRef](#)]

26. Khan, A.F.; Awais, M.; Khan, A.S.; Tabassum, S.; Chaudhry, A.A.; Rehman, I.U. Raman Spectroscopy of Natural Bone and Synthetic Apatites. *Appl. Spectrosc. Rev.* **2013**, *48*, 329–355. [[CrossRef](#)]
27. Xu, B.; Poduska, K.M. Linking Crystal Structure with Temperature-Sensitive Vibrational Modes in Calcium Carbonate Minerals. *Phys. Chem. Chem. Phys.* **2014**, *16*, 17634–17639. [[CrossRef](#)]

**Disclaimer/Publisher's Note:** The statements, opinions and data contained in all publications are solely those of the individual author(s) and contributor(s) and not of MDPI and/or the editor(s). MDPI and/or the editor(s) disclaim responsibility for any injury to people or property resulting from any ideas, methods, instructions or products referred to in the content.